Comparison of some properties of Y123 and Gd123 superconducting material

Thitipong Kruaehong[a, *], Supphadate Sujinnapram[b], Tunyanop Nilkamjon[c], Sermsuk Ratreng[c], Pongkaew Udomsamuthirun[c]

[a] Department of industrial electric, Faculty of Science and Technology, Suratthani Rajabhat University, Suratthani, 84100 Thailand.
[b] Department of Physics, Faculty of Liberal Arts and Science, Kasetsart University, Kamphaeng Saen Campus, Nakhon Pathom, 73140 Thailand.
[c] Prasarnmit Physics Research,Department of Physics, Faculty of Science, Srinakharinwirot University, Bangkok, 10110 Thailand.

***Corresponding Author:** thitipong.kru@sru.ac.th
https://doi.org/10.55674/jmsae.v11i3.247680

Received: 21 February 2022 | **Revised:** 16 March 2022 | **Accepted:** 19 July 2023 | **Available online:** 1 January 2024

Abstract

Gd123 and Y123 superconducting materials were synthesized using the conventional solid-state reaction method, and their physical properties were compared. The critical temperature was determined based on the relationship between resistivity and temperature, and the average temperatures of Gd123 and Y123 were found to be 87.35K and 86.48K, respectively. The percentage of the superconducting compound and non-superconducting compound was determined using the Rietveld refinement method, which also revealed that the orthorhombic crystal structure belonged to the superconducting compound. The Gd123 sample had a higher proportion of the superconducting compound than the Y123 sample. EDX mapping analysis was used to investigate the composition of the samples, including the elements Y, Ba, Cu, and O, and the absence of impurities. The Gd123 and Y123 samples had melting points of 1,313K and 1,303K, respectively. The oxygen content of the samples was determined using the iodometric titration method, and the Gd123 and Y123 samples had oxygen contents of 6.68 and 6.58, respectively.

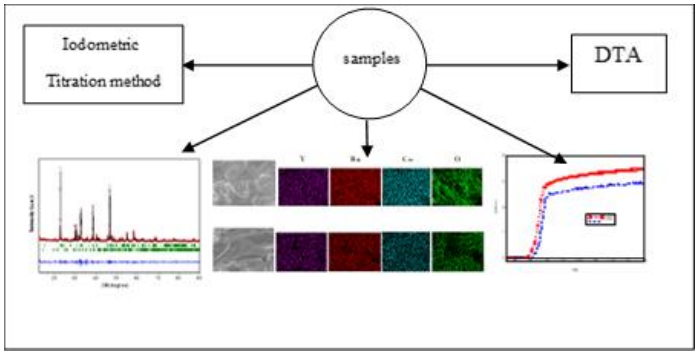

Keywords: Gd123; Y123; Four-probes measurement; X-ray diffraction

Introduction

Superconductivity is a phenomenon characterized by the absence of electrical resistance at a specific critical temperature (T_c). In 1986, Bednorz and Muller from IBM's laboratory [1] reported the development of a novel superconducting material known as La_2BaCuO_4 (La214) oxide, which exhibited a critical temperature exceeding 35 K. Achieving higher critical temperatures in the advancement of superconducting materials posed a significant challenge. The discovery of superconductivity in thin films of niobium-germanium [2], which demonstrated a critical temperature of 23.30 K when cooled with helium, necessitated the application of high pressures. In 1987, Chu et al. [3] reported the superconductivity of a ceramic compound comprising Yttrium, Barium, and copper oxide. This material showcased a critical temperature of approximately 93 K, attainable using relatively inexpensive liquid nitrogen cooling. The structural differences in the YBCO family, as well as the number of CuO_2 planes and CuO chains, result in a wide range of physical properties and critical temperatures. Y123 compounds have two CuO_2 planes and one CuO chain, with a T_c ranging from 92 − 94 K [4]. The crystal structure of Y123 is orthorhombic, characterized by three unequal perpendicular axes ($a \neq b \neq c$). The lattice parameters of Y123 further describe its crystal structure. For Y123, the measured lattice parameters are as follows: $a = 3.822$ Å, $b = 3.884$ Å, and $c = 11.69$ Å [5]. These

parameters define the lengths of the crystallographic axes, providing information about the overall shape and symmetry of the crystal lattice. The electrical properties and crystal structure of Y123 were analyzed in reference [6], providing a comprehensive understanding of the material. More recently, other ceramics have been documented, wherein the yttrium ion is substituted with various rare-earth elements, excluding Ce, Pr, Pm, and Tb. The resulting material, referred to as $REBa_2Cu_3O_7$-δ or "RE123" (RE: Nd, Sm, Eu, Gd, etc.), has emerged as the favored choice for numerous industrial applications. Enhancing the physical properties of RE123, such as critical current density (J_c) and critical magnetic field (H_c), at high temperatures around the boiling point of liquid nitrogen, has become the subject of extensive research. The rare-earth element Gd is utilized as a replacement for RE123, resulting in a superconductor known as Gd123.

The Gd123 superconducting material has emerged as a promising alternative in the field of high-temperature superconductors (HTSC). Its critical temperature transition occurs around 90 K [7], and it demonstrates the ability to trap magnetic fields up to 2 T at 77 K [8]. However, the current critical density shows an inverse relationship with the critical magnetic field. As the magnetic field increases, the J_c (critical current density) of Gd123 rapidly decreases due to the movement of non-superconducting vortices, particularly Gd211 (Gd_2BaCuO_5).In 2012, Huse et al. [9] synthesized bulk $Gd_{1-x}Pr_xBa_2Cu_3O_{7-\delta}$ superconductors through a solid-state reaction by introducing Pr as a substitution element. Gd_2O_3, $BaCO_3$, Pr_6O_{11}, and CuO were used as the initial powders. These powders were subjected to calcination at 1,188 K for 24 h in an air atmosphere, followed by intermediate grinding. The resulting powder underwent regrinding, pellet pressing, and sintering at 1,203 K for 24 h. Subsequently, annealing was carried out in an oxygen atmosphere at 723 K for 24 h. The structural analysis involved the use of an X-ray diffractometer with CuK_α radiation (λ=1.546 Å), and the electrical resistivity of the samples was measured using a four-probe method. The obtained physical properties revealed a critical temperature of 92.70 K and orthorhombic lattice parameters with a = 3.830 Å, b = 3.890 Å, and c = 11.680 Å. The crystal structure exhibited an oxygen content (δ) of 6.99.

In a more recent study, Basma et al. [10] employed the conventional solid-state reaction technique to synthesize samples of $(ZnFe_2O_4)_xGdBaCu_3O_{7-\delta}$ and $(CoFe_2O_4)_x GdBa_2Cu_3O_{7-\delta}$. The powders underwent calcination at 1,113 K and 1,153 K for 24 h in an air environment. Subsequently, the mixed powder was pressed into discs measuring 1.50 cm in diameter and 0.30 cm in thickness. The samples were sintered in air at 1,203 K for 24 h. X-ray diffraction (XRD) analysis was conducted to determine the phase composition of the samples. The results identified two phases: a superconducting phase and a non-superconducting phase. The lattice parameters of the superconducting phase were identified in an orthorhombic structure with a=3.840 Å, b=3.890 Å, and c=11.690 Å. Additionally, the presence of a second phase, $BaCuO_2$, with a cubic structure, was observed. For the samples with x=0, a critical temperature of 91.77 K was exhibited.

In 2019, Kruaehong et al. [11] studied the properties of superconductor Y123 by replacing the Y-atom with an Er-atom (Er123) in a solid-state reaction. The samples were subjected to a 24-hour thermal treatment at 1,223 K during calcination, followed by a 24-hour sintering at the same temperature. The resistivity versus temperature curves showed a single-step transition with a Tconset of 93 K. XRD analysis revealed an orthorhombic structure for the superconducting compound, with lattice constants of a = 3.820 Å, b = 3.880 Å, c = 11.680 Å, and an orthorhombicity parameter of 1.69%. In contrast, the non-superconducting compound exhibited a cubic structure with lattice constants of $a = b = c$ = 18.25 Å. A three-dimensional atomic position simulation was conducted. SEM micrographs showed large grain sizes and a uniform surface. EDX mapping confirmed a pure composition with smooth distributions of Er, Ba, Cu, and O elements. The heat reaction displayed an endothermic curve, with a peritectic temperature observed at 1277.980 K using DTA analysis. Cu^{2+} concentration was 6.30×10^{-6}, Cu^{3+} concentration was 1.82×10^{-6}, and the Cu^{3+}/Cu^{2+} ratio was 0.29. The oxygen deficiency, determined through a standard iodometric titration method, had a δ value of 0.16.

In this study, we explore the physical properties of the Gd123 compound, which was prepared using the conventional solid-state reaction method. The crystal structure of the material is determined by employing powder X-ray diffraction, and the lattice parameters of both the superconducting and non-superconducting compounds, along with their corresponding space groups, are characterized using the Reitveld refinement method. The superconductivity is evaluated through dc four-probe electrical resistivity measurements. The elemental composition is analyzed using mapping techniques, while the melting point is determined using Differential Thermal Analysis (DTA). Lastly, the oxygen content (δ) in the samples is examined using the standard iodometric titration method.

Materials and Methods

Samples of the chemical compounds $GdBa_2Cu_3O_{7-x}$ and $YBa_2Cu_3O_{7-x}$ were prepared through a conventional solid-state reaction method. High-purity powders of Gd_2O_3, Y_2O_3, $BaCO_3$, and CuO (with a purity of 99.99% from Aladdin) were thoroughly mixed and ground for 30 min. The mixture was then calcined at 1,223 K for 24 h in an air environment. This calcination process was repeated twice at 1,223 K for 24 h with intermediate grinding. Subsequently, the mixture was pressed into cylindrical pellets using an automatic press machine at a pressure of 1,500 psi. The resulting bulk samples were sintered at 1,223 K for 24 h. The samples were annealed in an oxygen environment at 773 K for 12 h, followed by slow cooling at a rate of 275.50 K min^{-1} to room temperature.

Table 1 displays the volume fraction and percentage of Gd123 and Y123. Gd123 has a superconducting compound percentage of 90.36%, whereas Y123 has a percentage of 85.46%. The non-superconducting compounds in Gd123 consist of $BaCuO_2$ and $Ba_2Cu_3O_6$, with respective percentages of 7.84% and 1.80%. In Y123, the non-superconducting compounds include Y_2BaCuO_5 (Y211), $BaCuO_2$, and $Ba_2Cu_3O_6$, with percentages of 6.35%, 3.15%, and 5.04% respectively. Comparing the volume fraction and percentage of the two samples, Gd123 exhibits a higher proportion of the superconducting compound compared to Y123. This discrepancy can be attributed to the larger atomic radius of Gd (233 pm) compared to Y (212 pm). Consequently, Gd123 showcases a greater prevalence of the superconducting compound relative to Y123.

Results and Discussions

40 min. At low temperatures of 150 °C, 200 °C, and 250 °C, respectively, cow fat could be partially dissolved. Fig. 5 shows the melted cow fat product at 69.67 wt.%, 72 wt.%, and 75 wt.%, respectively. There were also a lot of waxy materials and other suspended matter; however, it melted well to be 96.67 wt.% and 97.10 wt.% at high temperatures of 300 °C, 350 °C, respectively. Thus, there was very little wasted cow fat after the render fat down that was dark brown and very viscous, which the melted cow fat was called feedstock and FFA checks.

The amount of FFAs was important for alkaline transesterification, the FFA level in the oil should be below a desired level (ranging from less than 0.50% to less than 3%) [13]. From Fig. 6, the trend toward the increased temperature to render fat down also affected the higher FFA. As a consequence, the resulting soaps could induce an increase in viscosity, formation of the gels, and made the separation of glycerol difficult [8]. The temperatures at 150 °C, 200 °C, 250 °C, and 300 °C, respectively still resulted in the FFA having low range values of less than 1.50%. On the other hand, at a temperature of 350 °C, this resulted in a higher range of 2.53% of the FFA, and the major problem associated with processing low-cost fats and oils was that they had high quantities of FFAs that could not be easily transformed into biodiesel fuel by conventional alkali-catalyzed transesterification [18].

The lattice parameters of the superconducting compounds were determined through Reitveld refinement and are listed in Table 2. Gd123 exhibited lattice parameters of a=3.843 Å, b=3.900 Å, and c=11.70 Å, while Y123 had lattice parameters of a=3.821 Å, b=3.884 Å, and c=11.69 Å. The numbers below the lattice parameters represent the experimental error. The a and b lattice parameters for Gd123 and Y123 were similar, but the most noticeable disparity was observed in the *c* lattice parameter, with Gd123 having a longer value than Y123. The presence of porosity in the samples was indicated by the anisotropic parameter, which reflects the extent of structural variation. Y123 exhibited a higher anisotropic parameter compared to Gd123. This can be attributed to the smaller atomic radius of Y, which facilitates easier vibration within the crystal structure. As a result, Gd123 exhibits a more stable crystal structure compared to Y123.The miller indice of superconducting phase of Gd123 and Y123 were (003), (103), (010),(113) and (026) correspond to 2θ at 23°, 32°,38°,40° and 69°, respectively.

Table 1 Showsthe volume fraction of percentage of superconducting compound and non-superconducting compound of Gd123 and Y123.

Samples	Superconducting Compound	Non-superconducting Compound		
		Y_2BaCuO_5(Y211)	$BaCuO_2$	$Ba_2Cu_3O_6$
Gd123	90.36	-	7.84	1.80
Y123	85.46	6.35	3.15	5.04

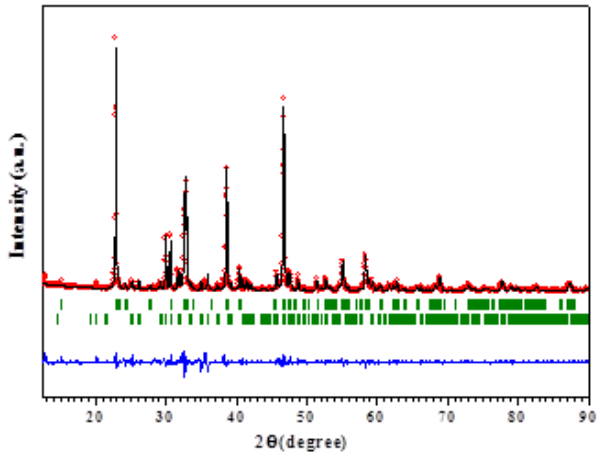

Fig. 1 XRD pattern for Gd123.

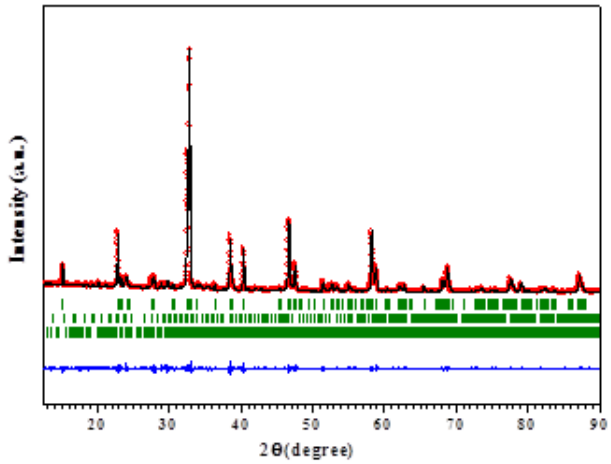

Fig. 2 XRD pattern of Y123.

In 2020, Agil and Akduran [12] synthesized Gd123 polycrystalline material using the solid-state reaction method. X-ray diffraction analysis was employed to determine the crystal structure, revealing that the superconducting phase of Gd123 exhibited an orthorhombic structure with Pmmm symmetry. The lattice parameters of the superconducting phase were measured as a = 3.839 Å, b = 3.893 Å, and c = 11.68 Å. Huse et al. [13] focused on the effect of Pr substitution in Gd123 superconductors. X-ray diffraction patterns of the samples without Pr doping showed an orthorhombic structure. The lattice constants a and b ranged between 3.891 Å and 3.898 Å, while the c lattice parameter was determined to be 11.49 Å. The orthorhombic distortion or anisotropic parameter was calculated as 1.511. Sujinnapram et al. [14] synthesized new YBaCuO superconductors using the solid-state reaction method. The crystal structure of YBaCuO was investigated using X-ray diffraction with CuKα radiation. The crystal structure and space group were refined using the Fullprof program. The superconducting phase, Y123, accounted for 94% of the composition and exhibited Pmmm symmetry, while the non-superconducting phase constituted 6% and displayed Pbnm symmetry. The lattice parameters of the superconducting phase were determined as a = 3.822 Å, b = 3.884 Å, and c = 11.69 Å.

The non-superconducting phase had lattice parameters of a = 7.140 Å, b = 12.19 Å, and c=5.652 Å. The X-ray diffraction spectra display peaks representing the non-superconducting compounds, although these peaks are smaller in comparison to those of the superconducting compounds. Gd123 exhibits two types of non-superconducting compounds. $BaCuO_2$, with a cubic lattice structure and belonging to the Im-3m space group, and $Ba_2Cu_3O_6$, which has an orthorhombic structure and falls under the Pccm space group. In the case of Y123, there are three types of non-superconducting compounds. Two of them, Y211 (Pbnm) and $Ba_2Cu_3O_6$ (Pccm), exhibit orthorhombic structures, while $BaCuO_2$ displays a cubic structure (Im-3m).

In the typical synthesis of Gd123 superconductors, Gd_2O_3, $BaCO_3$, and CuO are used as starting chemicals. Similarly, Y123 superconductors are synthesized using Y_2O_3, $BaCO_3$, and CuO. The combination of these starting chemicals results in the formation of Gd123 and Y123 phases at temperatures above 1,173 K [15]. Furthermore, the non-superconducting compounds Y_2BaCuO_5, $BaCuO_2$, and $Ba_2Cu_3O_6$ were examined through XRD analysis at 1,073 K in Table 3. However, Y123 can be produced from the non-superconducting compounds $BaCuO_2$ and Y_2BaCuO_5 at temperatures exceeding 1,173 K. Similarly, Gd123 can be produced from the non-superconducting compounds $BaCuO_2$ and Gd_2BaCuO_5 at the same temperature as Y123.

EDX mapping was utilized to identify and visualize all the elements present in Fig. 3 and 4. The procedure generated images, with the first one capturing the surface and showing the distribution of each element. Y, Ba, Cu, and O were represented by the colors pink, red, blue, and green respectively in the image. Comparing the surfaces of Gd123 and Y123, Gd123 displayed greater homogeneity, larger grain size, and a smoother surface in contrast to Y123. The distribution of elements in Gd123 appeared to be smoother than in Y123. The smooth and dense nature of the surface influenced electron transfer during the EDX mapping experiment.

Each element's image obtained through EDX mapping exhibited distinct characteristic X-ray signals. The results of the EDX mapping facilitated the identification of these characteristic X-rays. Specifically, the K_α X-ray line was used to identify Cu and O, while Gd and Ba were identified

using the Lα X-ray line. Spectra were examined to investigate the samples for any signs of contamination.

The temperature dependence of the electrical resistivity for Gd123 and Y123 is illustrated in Fig. 5. Temperature measurements were performed using a type K thermocouple within the range of 77 − 120 K. The thermocouple provided stable temperature control with a resolution of 1 K, and each temperature point had a response time of 15 min. The transition temperature behavior can be observed in three steps.

Step 1, known as the "hand of superconductivity," represents the state where the materials exhibit zero resistivity and is denoted by T_c offset(K). Step 2, referred to as the "hand of transition," signifies the transition from zero resistivity to the normal state and is denoted by T_c onset(K). Step 3, labeled as the "hand of the normal state," corresponds to the material's normal state.

To transition the samples from the superconducting state to the normal state, a closed cryogenic refrigeration system utilizing liquid nitrogen was utilized. The samples were connected to four copper leads using conductive silver paint. Simultaneous voltage and temperature measurements were performed using a Fluke 6.50-digit multimeter. The applied current density was 2.55 mA m^{-2}. The "hand of superconductivity" for all samples began at 77 K, and the offset critical temperature (T_c offset) marked the end of this state. The onset critical temperature (T_c onset) represented the end of the "hand of transition." The results indicated that Gd123, represented by the red graph, had a T_c offset of 82.96 K and a T_c onset of 89.76 K. Y123, represented by the blue graph, exhibited a T_c offset of 82.96 K and a Tc onset of 90 K, as presented in Table 4 and Fig. 5.

Analyzing the three states of the materials, it was observed that Y123 had a longer duration of the "hand of superconductivity" compared to Gd123. Thus, Y123 maintained its superconducting state better than Gd123. The difference in Tc offset between the two samples was 1.99 K. Additionally, Y123 displayed a shorter "hand of transition" compared to Gd123, with a difference of 0.24 K in the onset critical temperature. The average critical temperature was 87.35 K for Gd123 and 86.48 K for Y123, resulting in a discrepancy of 0.87 K in the average critical temperature. The closely measured critical temperature values determined the critical temperature of the two samples [15]

Table 4 The critical temperature of samples.

Samples	T_c offset (K)	T_c onset (K)	T_c average (K)
Gd123	84.95	89.76	87.35
Y123	82.96	90.00	86.48

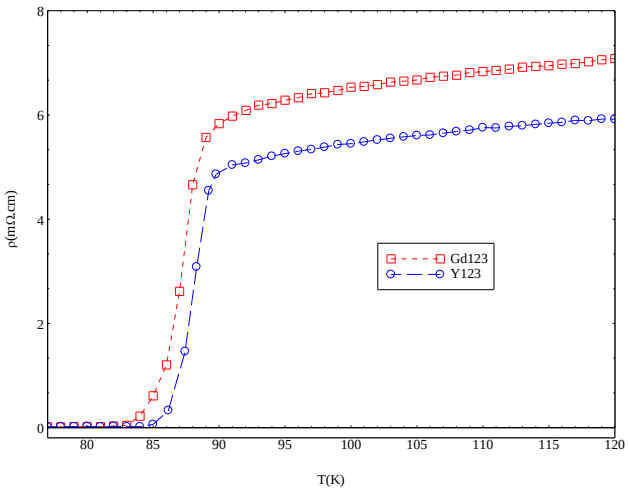

Fig. 5 Electrical resistivity dependence temperature of Gd123 and Y123.

In 2017, Kruaehong et al. conducted a synthesis and characterization study on Y123 superconductor using planetary high-energy ball milling. The Y123 bulk sample was synthesized through a solid-state reaction, and its critical temperature (T_c) was measured using the conventional standard four-probe technique. The milled sample exhibited a temperature of 92.68 K, while the unmilled sample showed a temperature of 93.00 K. The critical temperature of Y123 was improved by employing the planetary high-energy ball milling method, which enhanced the homogeneity of the sample powder.

In another study by Udomsamuthirun et al., various YBaCuO superconductors, including Y123, Y3-8-11, Y358, Y5-8-13, Y7-11-18, and Y13-20-33, were synthesized using the solid-state reaction method. The critical temperature was measured using the four-probe method, with the onset critical temperature of Y123 determined to be 93 K. During the synthesis process of Gd123 and Y123, the highest temperature reached was 1,223 K. X-ray diffraction results indicated the presence of non-superconducting compounds, such as Y211 (Y_2BaCuO_5), $BaCuO_2$, and $Ba_2Cu_3O_6$, at this temperature. However, these non-superconducting compounds were not detected in the actual samples. Some minor changes were observed in the samples at high temperatures during the synthesis process. The melting point of the samples was determined using Differential Thermal Analysis (DTA), with a temperature range of 1,073 − 1,473 K and a heating rate of 275 K min^{-1}. The DTA analysis revealed an endothermic heat reaction and melting points of 1,313 K for Gd123 and 1,303 K for Y123. In 2019, Zhang et al. investigated the melting temperature of Gd123 powder

Table 2 Lattice parameters of superconducting compound and anisotropic parameter of Gd123 and Y123.

Samples	Non-superconducting Compound			Anisotropic parameters = 200 (*b*-*a*)/(*b*+*a*)
	a(Å)	*b*(Å)	*c*(Å)	
Gd123	3.84	3.89	11.70	1.37
	0.05	0.03	0.18	
Y123	3.82	3.88	11.68	1.62
	0.07	0.05	0.15	

obtained from Shanghai Superconductor Technology Co., Ltd., and found the melting point of Gd123 to be 1,315 K after heat treatment in air within a temperature range of 1,073 − 1,673 K.

Both Gd123 and Y123 are oxide compound superconductors with a crystal structure consisting of Cu-O chains and CuO_2 planes in their unit cells. Electron transfer within the crystal structure occurs through hole pumping in the CuO_2 planes. The crystal structures of Gd123 and Y123 share similarities, with one Cu-O chain and two CuO_2 planes. The oxygen content in the samples plays a crucial role as it affects the critical temperature and electron transfer within the crystal structure. The oxygen content was determined using the Iodometric Titration method, and it ranged from 6.50 − 7. Oxygen contents above 6.50 indicate non-superconducting materials, while values below 6.50 suggest variations in critical temperature. The results showed an oxygen content of 6.687 for Gd123 and 6.585 for Y123, respectively. The oxygen content influences the different physical properties of the samples.

Conclusion

The polycrystalline Gd123 and Y123 materials were prepared using the conventional solid-state reaction method. The crystal structure of the samples was investigated through X-ray diffraction and Rietveld refinement procedures. The samples contained a combination of superconducting and non-superconducting phases. The superconducting phase accounted for % in Gd123 and % in Y123, while the non-superconducting phase made up the remaining percentage. The superconducting phase exhibited an orthorhombic structure with Pmmm symmetry.

In Gd123, the non-superconducting phase consisted of $BaCuO_2$ (Im-3m) and $Ba_2Cu_3O_6$ (Pccm), whereas in Y123, it included Y_2BaCuO_5 (Pbnm), $BaCuO_2$, and $Ba_2Cu_3O_6$ (Pccm). EDX mapping provided insights into the distribution of Y, Ba, Cu, and O in the samples, confirming the absence of impurities. The average critical temperatures were determined using the four-probe method, resulting in 87.35 K for Gd123 and 86.48 K for Y123. The melting point was found to be 1,313 K for Gd123 and 1,303 K for Y123. The oxygen content, determined by the Iodometric titration method, was measured to be 6.68 for Gd123 and 6.58 for Y123.

Acknowledgement

The assistance provided by the Research and Development Institute of Suratthani Rajabhat University partially supported this work. The Department of Physics at Srinakharinwirot University is recognized for their contribution.

References

[1] J.G. Bednorz, K.A. Muller, Possible High Tc Superconductivity in the Ba-La-Cu-OSystem, Z. Phys. B 64 (1986) 189 − 193.

[2] C. Arkadiusz, S. Lukasz, T. Marek, G. Ewa, T. Pawel, S. Tomasz, Evidence ofGermanium segregation in Gold Thin Films, Surf. Sci. 674 (2018) 73 − 78.

[3] K. Wu, J.R. Ashburn, C.J. Torng, P.H. Hor, R.L. Meng, L. Gao, Z.J. Huang, Y.Q. Wang, C.W. Chu, Superconductivity at 93 K in a New Mixed-Phase Y-Ba-Cu-O Compound System at Ambient Pressure, Phys. Rev. Lett. 58 (1987) 908 − 910.

[4] S. Gholipour, V. Daadmehr, A.T. Rezakhani, H. Khosroabadi, F.S. Tehrani, R.H. Akbarnejad, Y358 against Y123 structural phase in a Y-based superconductor, arXiv preprint. (2011) 1110.0893.

[5] T. Kruaehong, Investigate the characterization of y7-11 − 18 superconductor, The 2nd International Conference on Applied Science (ICAS), The 3rd International Conference on Science and Technology for Sustainable Development of the Greater Mekong Sub-region(STGMS) Souphanouvong University, Luang Prabang, Lao PDR. (2011) 24 − 25.

[6] T. Kruaehong, Electrical properties and crystal structure of Y123, Y358 and Y257/Y211 composite

bulk superconductors, Int. J. Phys. Sci. 9(16) (2014), 360 − 367.

[7] Y. Xu, K. Tsuzuki, S. Hara, Y. Zhang, Y. Kimura, M. Izumi, Spatial variation ofSuperconducting Properties of Gd123 Bulk superconductors with Magnetic ParticlesAddition, Physica C. 470 (2010) 1219 − 1223.

[8] O. Yuta, K. Takanobu, G. Suguru, I. Kazutaka, H. Kohei, I. Masayoshi, Y. Masateru, I. Teruo, Critical Current Density in Gd1Ba2Cu3O7-δ Coated Conductor Under theInfluence of Flux Creep, Phys Proc. 67 (2015) 926 − 930.

[9] V. Huse, V. Mote, Y. Purushotham, B. Dole, Synthesis and Characterization of Pr substituted Gd-123 High-TcSuperconductors, Ceramica. 58 (2012) 381 − 387.

[10] M.B. Hadi, S. Isber, S. Noureldeen, A. Mohammed, EPR studies for GdBa2Cu3O7-δ added with nanosized ferrite CoFe2O4, Front. Theo. Appl. Phys, 869(2017) 1 − 4.

[11] T. Kruaehong, S. Sujinnapram, P. Udomsamuthirun, Superconductivity and Structural of ErBa2Cu3O7-δ Bulk Superconductor, J. Mater. Sci. Appl. Energy. 8(3) (2019) 460 − 468.

[12] H. Agil and N. Akduran, Structural, Electrical and Magnetics of FeO added GdBaCuO Superconductors, Adv. J. Sci. Eng. 1(4) (2020) 122 − 127.

[13] V.R. Huse, V.D. Mote, Y. Purushotham, B.N. Dole, Synthesis and Characterization of Pr substitutedGd-123 high-T Superconductors, Ceramica. 58 (2012) 381 − 387.

[14] S. Sujinnapram, P. Udomsamuthirun, T. Kruaehong, T. Nilkamjon, S. Ratreng. XRD Spectra of new YBaCuO Superconductors, Bull. Mater. Sci, 34 (2011) 1053 − 1057.

[15] N.H. Babu, I. Kazumasa, B. Amy, S. Yun-Hua, S.M. Lee, C. David, Bulk Superconducting Nano-Composites With High Critical Currents, IEEE Trans. Appl. Supercond. 17(2) (2007) 2953 − 2956.

[16] B. Li, K.Xu, S. Hara, D. Zhou, Y. Zhang, M. Izumi, Enhanced Pinning Effect in Air-Processed Gd-123 Bulk Superconductors with $BaTiO_3$ addition, Physica C. 475 (2012) 51 − 56.

[17] T.Kruaehong, S.Sujinnapram, T.Nilkamjon,S.Ratreng, P.Udomsamuthirun. Synthesized and Characterization of $YBa2CuO_7$, YBa5Cuand Y7Ba11Cu18Oy Superconductors by planetary high-energy ball-milling, J. Aust. Ceram. 53 (2017) 3 − 10.

[18] P. Udomsamuthirun, T. Kruaehong, T. Nilkomjon, S. Ratreng. The new Superconductors of YBaCuO Materials, J. Supercond. Nov. Magn.1377 − 1380.

[19] Z. Zhang, L. Wang, J. Liu, Q. Wang, Synthesis of ErBa2Cu3O7-δ Superconductor Solder for the Fabrication of Superconducting Joint between GdBa2Cu3O7-δ Coated Conductor, Crystals. 9 (2019) 492 − 501.